2016

A 9-bit multiple relaxation Lattice Boltzmann magnetohydrodynamic algorithm for 2D turbulence

Christopher Flint
William & Mary

George Vahala
William & Mary

Linda Vahala

Min Soe

Recommended Citation

Flint, Christopher; Vahala, George; Vahala, Linda; and Soe, Min, A 9-bit multiple relaxation Lattice Boltzmann magnetohydrodynamic algorithm for 2D turbulence (2016). *Computers & Mathematics with Applications*, 72(2), 394-403.
10.1016/j.camwa.2015.09.008

A 9-bit multiple relaxation Lattice Boltzmann Magnetohydrodynamic Algorithm for 2D Turbulence

Christopher Flint [1], George Vahala [1], Linda Vahala [2] and Min Soe [3]

[1] Department of Physics, William & Mary, Williamsburg, VA 23187
[2] Department of Electrical & Computer Engineering, Old Dominion University, Norfolk, VA 23529
[3] Department of Mathematics and Physical Sciences, Rogers State University, Claremore, OK 74017

Abstract

While a minimalist representation of 2D Magnetohydrodynamics (MHD) on a square lattice is a 9-bit scalar and 5-bit vector distribution functions, here we examine the effect of using the 9-bit vector distribution function on the effect of a magnetic field on the Kelvin-Helmholtz instability. While there is little difference in the simulation results between the 5-bit and the 9-bit vector distribution models in the vorticity, energy spectra.., the 9-bit model permits simulations with mean magnetic field a factor of approximately $\sqrt{2}$ greater than those attainable in the standard 5-bit model. Indeed a 9-bit single-relaxation model can attain such success over a 5-bit multiple-relaxation model at the same computational expense.

Keywords: Lattice Botzmann; MHD;2D turbulence; single and multiple relaxation

1. Introduction

Lattice Boltzmann (LB) algorithms [1] are an extremely successful computational technique for solving nonlinear collisional problems because of their simplicity of coding and their ideal parallelization. In principle, one is replacing a computationally difficult problem involving nonlinear convective terms by a linearized kinetic equation with simple advection and local collision operator. Since one is now solving on a lattice in kinetic space, one typically reduces the inherited extra memory/calculations by minimizing the number of kinetic velocities required in LB to recover the fluid equations in the long wavelength limit. In particular, such a minimalist 2D LB MHD model has been introduced by Dellar [2]. It consists of a 9-bit square lattice model for the evolution of the quasi-incompressible fluid velocity **u** and a 5-bit (square lattice) model for the evolution of the magnetic field **B**. This asymmetry is because the fluid velocity **u** arises as the 1st moment but the magnetic field arises from the 0th moment of their corresponding distributions. Here we consider in some detail the effect of utilizing the same 9-bit square lattice for the vector magnetic distribution function as for the particle distribution function on the magnetic stabilization of the Kelvin-Helmholtz instability [3, 4]. In considering the stabilization of a velocity jet we extend the collision operator for the evolution of the vector magnetic distribution to a multiple relaxation model (MRT) – a relaxation model introduced in 2002 by d'Humieres et. al [5] for LB for Navier-Stokes flows and which permitted numerically stable LB simulations for considerably higher flow velocities than could be achieved by the single relaxation rate (SRT). Similarly, we [6] have found that an MRT extension to the evolution of the 5-bit vector distribution function permitted considerably greater **B**-fields than under the SRT collision operator. [We note that MRT models for LB MHD have also been considered earlier by Dellar [9, 10], but these papers were not concerned with the question we are investigating]. Here we will find that even a single relaxation rate (SRT) model of the 9-bit collision operator leads to stable simulations with magnetic field magnitudes on the order of 34% greater than those attainable from the 5-bit MRT simulations at fixed Reynolds numbers. Moreover, this can be achieved at the same computational expense (wallclock time). Moving to 9-bit MRT model only gains a further 6% in maximum B-field over the 9-bit SRT, but with a wallclock time increase of over 50%. These results have direct bearing on LB-MHD tokamak simulations with its much larger toroidal to poloidal magnetic fields.

2. Lattice Boltzmann Algorithms

For 2D LB MHD [2], the minimalist square lattice is 9 streaming velocities for the evolution of the scalar density distribution function, Fig. 1, but 5 streaming velocities for the vector magnetic distribution $[\mathbf{e}_i, i = 0....4]$. However, here we will consider using exactly the same kinetic lattice velocities for both distributions – the D2Q9 model.

The lattice vectors are along the axes and the diagonals of a unit square

$$\mathbf{e}_i = \left(0,0\right), \left(\pm 1, 0\right), \left(0, \pm 1\right), \ \left(\pm 1, \pm 1\right) \ , \quad i = 0 \ldots 8 \tag{1}$$

The 2-step SRT lattice algorithm (with relaxation rate τ) for the scalar distribution $f_i\left(\mathbf{x},t\right)$ consists of a stream-collide sequence

$$\text{Stream:} \quad \mathrm{f}_i'\left(\mathbf{x}, t+\delta t\right) = \mathrm{f}_i\left(\mathbf{x} - \mathbf{e}_i \delta t, t\right)$$

$$\text{Collide:} \quad \mathrm{f}_i\left(\mathbf{x}, t+\delta t\right) = \mathrm{f}_i'\left(\mathbf{x}, t+\delta t\right) + \frac{1}{\tau}\left(\mathrm{f}_i^{eq}\left(\rho, \mathbf{u}, \mathbf{B}\right) - \mathrm{f}_i'\left(\mathbf{x}, t+\delta t\right)\right) \tag{2}$$

where the streaming is a shift of the data from one spatial lattice node to a neighboring node, while

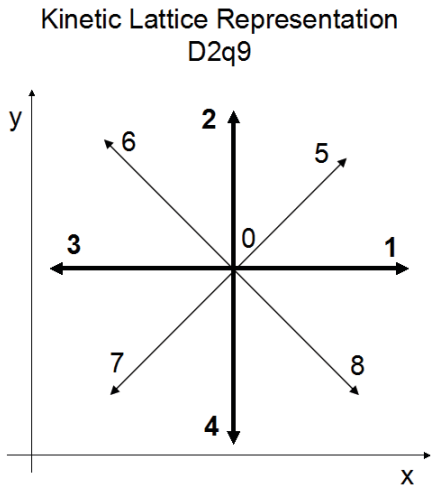

Fig. 1 The D2Q9 velocity lattice for our 2D LB-MHD simulations.

where the streaming is a shift of the data from one spatial lattice node to a neighboring node, while the collision step requires only local on-site information. Similarly, for the SRT evolution of the vector magnetic distribution $\mathbf{g}_i(\mathbf{x},t)$

$$\text{Stream:}\quad \mathbf{g}_i'(\mathbf{x},t+\delta t)=\mathbf{g}_i(\mathbf{x}-\mathbf{e}_i\delta t,t)$$

$$\text{Collide:}\quad \mathbf{g}_i(\mathbf{x},t+\delta t)=\mathbf{g}_i'(\mathbf{x},t+\delta t)+\frac{1}{\tau_m}\left(\mathbf{g}_i^{eq}(\rho,\mathbf{u},\mathbf{B})-\mathbf{g}_i'(\mathbf{x},t+\delta t)\right),\quad i=0....8 \qquad (3)$$

From Chapman-Enskog theory, the kinetic equations (2) and (3) are coupled through the **u-** and **B-** fields in the relaxated distributions, f^{eq} *and* $\mathbf{g}^{eq}$ [2]

$$\mathrm{f}_i^{eq}=w_i\rho\left[1+3(\mathbf{e}_i\cdot\mathbf{u})+\tfrac{9}{2}(\mathbf{e}_i\cdot\mathbf{u})^2-\tfrac{3}{2}\mathbf{u}^2\right]+\tfrac{9}{2}w_i\left[\tfrac{1}{2}\mathbf{B}^2\mathbf{e}_i^2-(\mathbf{B}\cdot\mathbf{e}_i)^2\right]+O(\mathbf{u}^4),$$

$$\mathbf{g}_i^{eq}=w_i\left[\mathbf{B}+3\left\{(\mathbf{e}_i\cdot\mathbf{u})\mathbf{B}-(\mathbf{e}_i\cdot\mathbf{B})\mathbf{u}\right\}\right]+O(\mathbf{u}^4), \qquad (4)$$

with the same *weights* $w_0=\frac{4}{9},w_{1\ldots4}=\frac{1}{9},w_{5\ldots8}=\frac{1}{36}$

Lattice Boltzmann Moments [7,8]

The 0th and 1st moments of the scalar distribution function yield the density and momentum of the fluid, while the 0th moment of the vector distribution function yields the magnetic field

$$\rho=\sum_{i=0}^{8}f_i(\mathbf{x},t)\ ,\quad \rho\,\mathbf{u}=\sum_{i=0}^{8}\mathbf{e}_i f_i(\mathbf{x},t)\quad ;\quad \mathbf{B}=\sum_{j=0}^{8}\mathbf{g}_j(\mathbf{x},t) \qquad (5)$$

One now constructs an orthogonal basis :

$$M_i=\sum_{j=0}^{8}\Psi_{ij}f_j\quad ;\quad N_{i\beta}=\sum_{j=0}^{8}\psi_{ij}\,g_{j\beta}\ ,\quad i=0....8\ ;\ \beta=x,y \qquad (6)$$

using the 9-vectors for the velocity distribution

$$c_x=\{0,1,0,-1,0,1,-1,-1,1\}\ ,\ c_y=\{0,0,1,0,-1,1,1,-1,-1\}$$

with $(j = 0....8)$

$$\Psi_{0j} = 1 \quad , \quad \Psi_{1j} = c_x \quad , \quad \Psi_{2j} = c_y \quad , \quad \Psi_{3j} = c_x c_y \quad , \quad \Psi_{4j} = c_x^2 - c_y^2 \, , \, \Psi_{5j} = 3c_x c_y^2 - 2c_x$$

$$\Psi_{6j} = 3c_x^2 c_y - 2c_y \, , \Psi_{7j} = 4 - 9\left(c_x^2 + c_y^2 - 2c_x^2 c_y^2\right), \; \Psi_{8j} = 4 - 4\left(c_x^2 + c_y^2\right) + 3\, c_x^2 c_y^2$$

and

$$\psi_{0j} = 1 \; , \; \psi_{1j} = c_X \, , \; \psi_{2j} = c_Y \, , \quad \psi_{3j} = c_X^2 \; , \; \psi_{4j} = c_Y^2 \quad ,$$
$$\psi_{5j} = c_X c_Y \quad , \; \psi_{6j} = c_X^2 c_Y \, , \; \psi_{7j} = c_X c_Y^2 , \quad \psi_{8j} = c_X^2 c_Y^2 \quad , \; j = 0...8 \qquad . (7)$$

We can now determine a new set of orthogonal moments whose equilibria are the 5 conserved moments (collisional invariants for quasi-incompressible MHD)

$$M_0 = \rho \quad , \quad M_1 = \rho u_x \; , \; M_2 = \rho u_y \quad ; \quad N_{0\beta} = B_\beta \triangleq N_\beta \, , \, \beta = x,y \qquad (8)$$

and the equilibria moments (with the M's corresponding to the fluid moments and the N's corresponding to magnetic field moments)

$$M_3^{eq} = \frac{M_1 M_2}{M_0} - N_x N_y \quad ; \quad M_4^{eq} = \frac{M_1^2 - M_2^2}{M_0} - N_x^2 + N_y^2 \quad ; \; M_5^{eq} = -M_1$$

$$M_6^{eq} = -M_2 \quad ; \; M_7^{eq} = -3\frac{M_1^2 + M_2^2}{M_0} \quad ; \quad M_8^{eq} = \frac{5}{3}M_0 - 3\frac{M_1^2 + M_2^2}{M_0} \qquad . \qquad (9)$$

$$N_{1\beta}^{eq} = \frac{N_{0\beta} M_x - N_{0x} M_\beta}{M_0} \quad ; \quad N_{2\beta}^{eq} = \frac{N_{0\beta} M_y - N_{0y} M_\beta}{M_0} \quad ; \quad 3N_{3\beta}^{eq} = N_{0\beta} \; ; \quad 3N_{4\beta}^{eq} = N_{0\beta}$$

$$N_{5\beta}^{eq} = 0 \quad ; \quad 3\, N_{6\beta}^{eq} = N_{2\beta}^{eq} \; ; \quad 3N_{7\beta}^{eq} = N_{1\beta}^{eq} \quad ; \quad 9N_{8\beta}^{eq} = N_{0\beta} \; .$$

Thus the LB evolution in the velocity distribution basis would yield (say for i= 3 lattice direction)

$$\partial_t f_3 + \mathbf{e}_3 \bullet \nabla f_3 = \frac{1}{\tau}\left(f_3^{eq} - f_3\right)$$

while the evolution equation for the i = 3 moment yields

$$\partial_t M_3 + \frac{1}{3}\partial_x\left(2M_2 + M_6\right) + \frac{1}{3}\partial_y\left(2M_1 + M_5\right) \; = \; \frac{1}{\tau}\left(M_3^{eq} - M_3\right)$$

*div **B** = 0 in LB-MHD Algorithm*

In the Dellar [2] vector magnetic distribution function approach, one can enforce $\nabla \bullet \mathbf{B} = 0$ automatically. Reverting to Dellar's moment definitions

$$\left(N_{1\beta}, \, N_{2\beta}\right) \; = \Lambda_{\alpha\beta} \quad , \alpha = x,y$$

one finds that (for 9-bit magnetic lattice)

$$\partial_t \Lambda_{\alpha\beta}^{eq} + \partial_\gamma \sum_{i=0}^{8} e_{i\gamma} e_{i\gamma} g_{i\beta}^{eq} = -\frac{1}{\tau_m}\Lambda_{\alpha\beta}^{(1)} \quad , \quad with \;\; \Lambda_{\alpha\beta}^{(n)} = \sum_{i=0}^{8} e_{i\alpha} g_{i\beta}^{(n)} \qquad (10)$$

with the antisymmetric tensor

$$\Lambda_{\alpha\beta}^{eq} = u_\alpha B_\beta - B_\alpha u_\beta \qquad (11)$$

Since $\sum_{i=0}^{8} e_{i\gamma} e_{i\alpha} g_{i\beta}^{eq} = \delta_{\gamma\alpha} B_\beta$, one immediately obtains to leading order that $\Lambda_{\alpha\beta}^{(1)} = -\tau_m \partial_\alpha B_\beta$. On taking the trace one finds

$$Tr\left[\Lambda_{\alpha\beta}^{(1)}\right] = -\tau_m \nabla \bullet \mathbf{B} + O\left(Ma^3\right) \quad , \text{ with } \quad Ma = \text{Mach number.} \tag{12}$$

From 2D LB-MHD turbulence studies [2, 6] of $\nabla \bullet \mathbf{B} = 0$, the moment $Tr\left[\Lambda_{\alpha\beta}^{(1)}\right]$, Eq. (10), is very

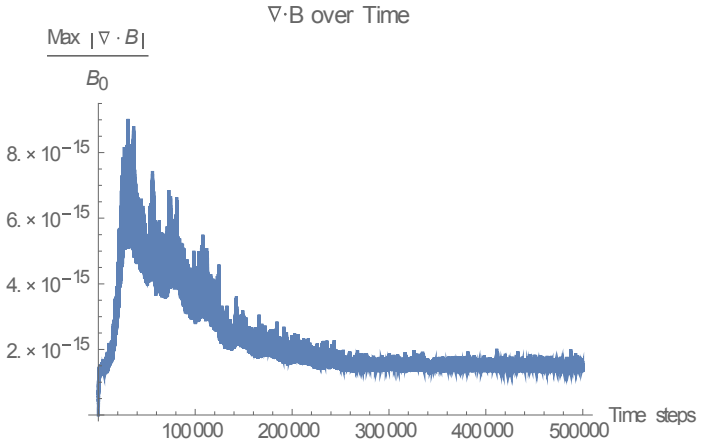

(a) D2Q5-MRT model for **B-**field

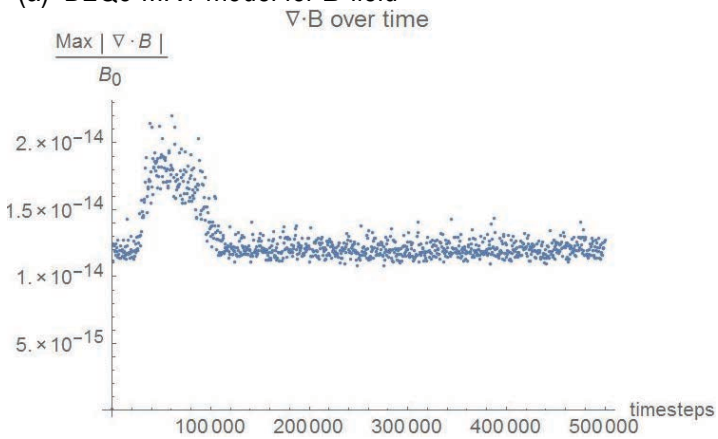

(b) D2Q9-SRT model for **B-**field

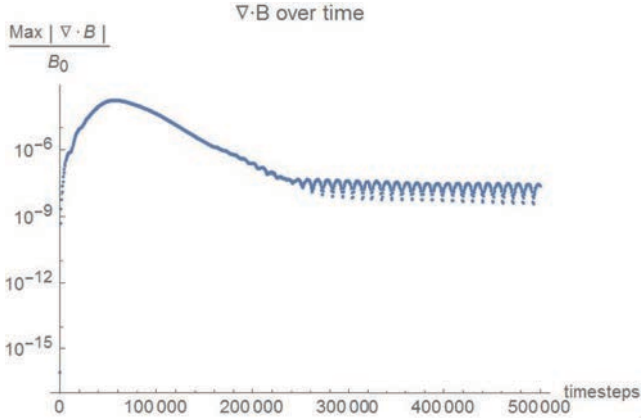

(c) D2Q9-MRT model for **B-**field

Fig. 2 The direct calculation of the perturbed moment $Tr\left[\Lambda^{(1)}_{\alpha\beta}\right]$*, which is related to div* ***B*** *by Eq. (12) for (a) D2Q5-MRT, (b) D2Q9-SRT, and (c) D2Q9-MRT lattice models for the evolution of the vector magnetic distribution function. Both D2Q5-MRT and D2Q9-SRT lattices preserve* $\nabla \bullet \mathbf{B} = 0$ *to extremely high precision. However in the D2Q-MRT model the perturbed moment asymptotes to a significantly higher level of* 10^{-8}*.*

close to zero for the D2Q5 lattice but, interestingly, only slightly higher for the D2Q9-SRT, but significantly higher for D2Q9-MRT model, Fig. 2.

3. Single Relaxation LB-MHD

In the single relaxation time (SRT) approach, all the moments have the same time relaxation rate – which for the fluid moments is τ and for the magnetic field moments is τ_m. We outline the derivation of the SRT magnetic field evolution equation. Under Chapman-Enskog expansions

$$\partial_t = \varepsilon\partial_t^{(0)} + \varepsilon^2\partial_t^{(1)} \quad , \quad \partial_\beta = \varepsilon\partial_\beta \quad , \quad \bar{M}_i = M_i^{eq}\left(\bar{M}_0, \bar{M}_1, \bar{M}_2, \bar{N}_x, \bar{N}_y\right) + \varepsilon\bar{M}_i^{(1)} \ .....$$

since the equilibrium moments can only be functions of the conserved moments. To leading order

$$\partial_t^{(0)} N_\alpha + \partial_\beta \Lambda^{eq}_{\beta\alpha} = 0$$

while at $O\left(\varepsilon^2\right)$

$$\partial_t^{(1)} N_\alpha + \partial_\beta\left[\left(1 - \frac{1}{2\tau_m}\right)\Lambda^{(1)}_{\beta\alpha}\right] = 0$$

Combining these two equations yields

$$\partial_t N_\alpha + \partial_\beta\left[\varepsilon\left(1 - \frac{1}{2\tau_m}\right)\Lambda^{(1)}_{\beta\alpha} + \Lambda^{eq}_{\beta\alpha}\right] = 0$$

But from the perturbed moments to leading order [c.f., Eq. (12)}: $\Lambda^{(1)}_{\alpha\beta} = -\frac{\tau_m}{3}\partial_\alpha N_\beta$.

After some straightforward manipulations one recovers the evolution equation for the magnetic field

$$\frac{\partial \mathbf{B}}{\partial t} = \nabla \times \left(\mathbf{u} \times \mathbf{B}\right) + \eta\nabla^2\mathbf{B} \tag{13}$$

with the resistivity

$$\eta = \frac{1}{3}\left(\tau_m - \frac{1}{2}\right) \tag{14}$$

Similarly for the fluid equations`

$$\frac{\partial \rho}{\partial t} + \nabla \cdot \rho\mathbf{u} = 0 \quad , \quad \frac{\partial \mathbf{u}}{\partial t} + \left(\mathbf{u} \cdot \nabla\right)\mathbf{u} = -\nabla \mathrm{P} + \left(\nabla \times \mathbf{B}\right) \times \mathbf{B} + \nu\left[\nabla\left(\nabla \cdot \mathbf{u}\right) + \nabla^2\mathbf{u}\right]$$

with the pressure in this isothermal model: $P = \rho/3$ and the viscosity

$$\nu = \frac{1}{3}\left(\tau - \frac{1}{2}\right) \tag{15}$$

4. Multiple Relaxation LB-MHD

The SRT model of LB-MHD becomes numerically unstable as one increases the Reynolds number $\left(\mathrm{Re} = U_0 L/\nu\right)$ and magnetic Reynolds number $\left(\mathrm{Re}_M = U_0 L/\eta\right)$. This bottleneck can be relieved if one proceeds to MRT in both kinetic equations. Of the 9 possible relaxation rates correlated to the 9 lattice vectors introduced in the evolution of the velocity distribution equation [5], several of these rates are fixed by the choice of the shear viscosity $\nu = \frac{1}{3}\left(\tau_3 - \frac{1}{2}\right) = \frac{1}{3}\left(\tau_4 - \frac{1}{2}\right)$, and the bulk viscosity [12] $\xi = -\frac{1}{9} - \frac{\tau_4}{9} - \frac{\tau_7}{15} + \frac{2\tau_8}{5}$

$$\frac{\partial \mathbf{u}}{\partial t} + \left(\mathbf{u}\cdot\nabla\right)\mathbf{u} = -\nabla \mathrm{P} + \left(\nabla\times\mathbf{B}\right)\times\mathbf{B} + \nu\left[\tfrac{2}{3}\nabla\left(\nabla\cdot\mathbf{u}\right) + \nabla^2\mathbf{u}\right] + \xi\nabla\left(\nabla\cdot\mathbf{u}\right)$$

This leaves three relaxation rates $\left(\tau_5, \tau_6, \tau_7\right)$ free for the stabilization of the LB-MHD algorithm without affecting the viscosity. We now proceed to the evolution of the magnetic field using the 9-bit model, rather than the usual 5-bit model of Dellar [2]. For the 9-bit SRT the single relaxation rate is determined by the resistivity. However, for the 9-bit MRT, It can be shown that the resistivity is determined by four of the magnetic distribution function relaxation rates,

$$\eta = \left(\tau_{M,1x} - \tfrac{1}{2}\right)/3 \;=\; \left(\tau_{M,1y} - \tfrac{1}{2}\right)/3 \;=\left(\tau_{M,2x} - \tfrac{1}{2}\right)/3 \;=\left(\tau_{M,2y} - \tfrac{1}{2}\right)/3$$

which leaves five free relaxation rates for the stabilization of the MHD equations. For some runs we have chosen all these free parameters as 0.625 [while those rates determining the transport coefficient are $\tau_3 = \tau_4 = 0.503$, $\tau_{M,1x} = \tau_{M,1y} = \tau_{M,2x} = \tau_{M,2y} = 0.50075$], while other runs we chose one of the relaxation rates to be 0.5 or 0.833 while the others were fixed at 0.625.

In the simulations below we will find that the 9-bit SRT magnetic field representation is more stable than the usual 5-bit MRT model and permits stronger mean fields by a factor of around 34% . It should be noted that Dellar [9, 10] has also introduced multiple relaxation collision operator for the evolution equation of the magnetic distribution function in 5-bit model – but in these papers only 2 collision rates are introduced.

5. MRT/SRT LB-MHD Simulation on Jet flow stabilization

Typically the Kelvin-Helmholtz instability [3, 4, 11] arises from velocity (or current) shear. In the absence of a magnetic field, the linear incompressible theory leads to the dispersion relation

$$\frac{\omega}{k} = \frac{1}{2}\left(U_1 + U_2\right) \pm i\frac{1}{2}\left|U_1 - U_2\right| \tag{16}$$

where U_1, U_2 are the representative velocities in the shear layer. Hence the linear perturbation is always unstable. If there is a uniform magnetic field parallel to the fluid velocity, this dispersion relation changes to

$$\frac{\omega}{k} = \frac{1}{2}\left(U_1 + U_2\right) \pm \sqrt{\frac{B_0^2}{\rho_0} - \frac{1}{4}\left(U_1 - U_2\right)^2} \tag{17}$$

Thus this instability can be stabilized for sufficiently strong magnetic field if the Alfven speed

$$V_A = B_0 / \sqrt{\rho_0} \; > \frac{1}{2}\left|U_1 - U_2\right|.$$

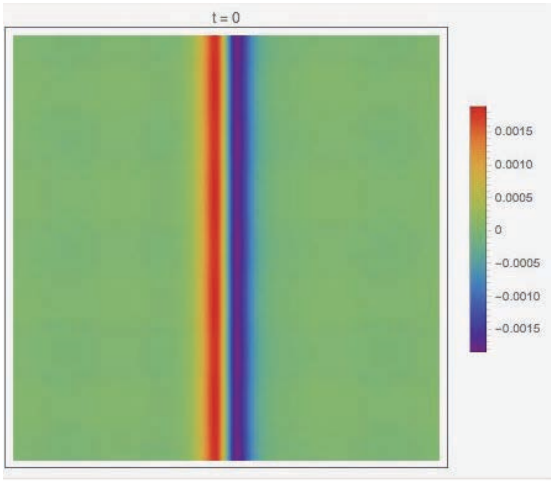

(a) t = 0

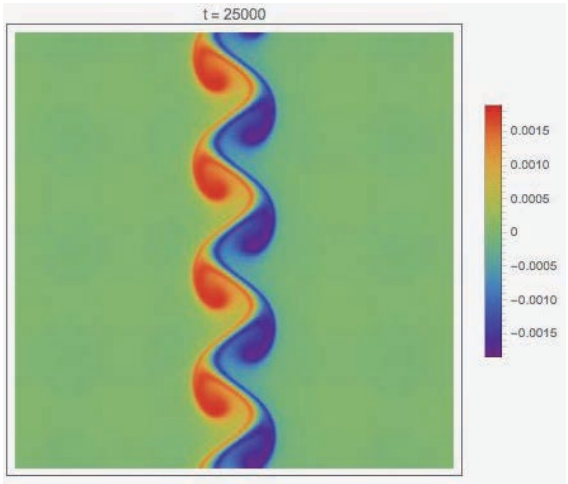

(b) t = 25 x 10^3

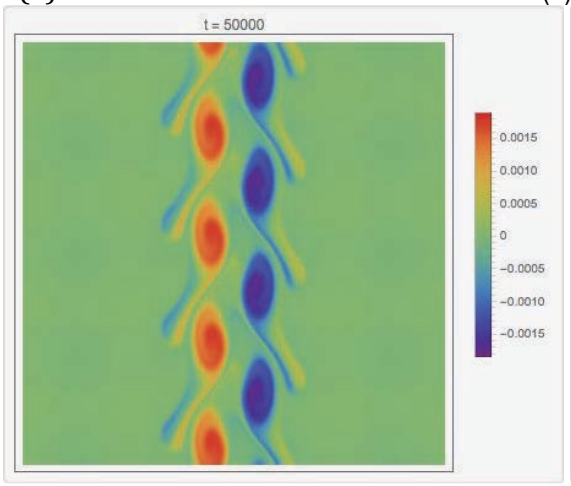

(c) t = 50 x 10^3

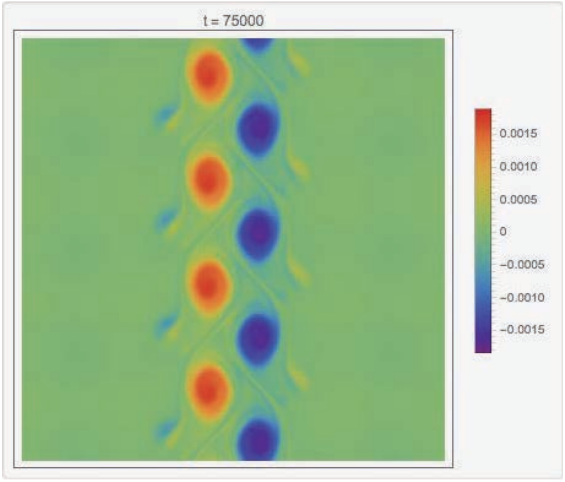

(d) t = 75 x 10^3

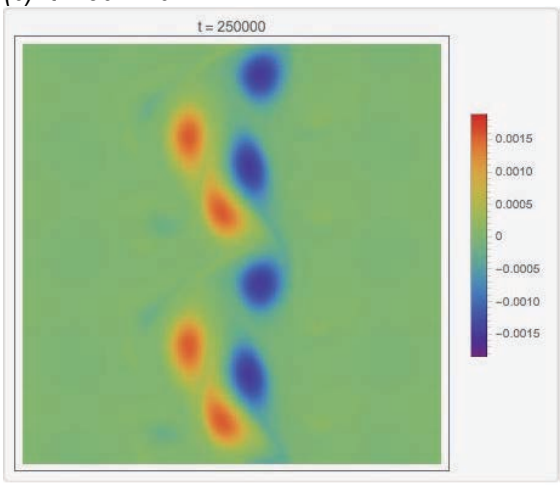

(d) t = 250 x 10^3

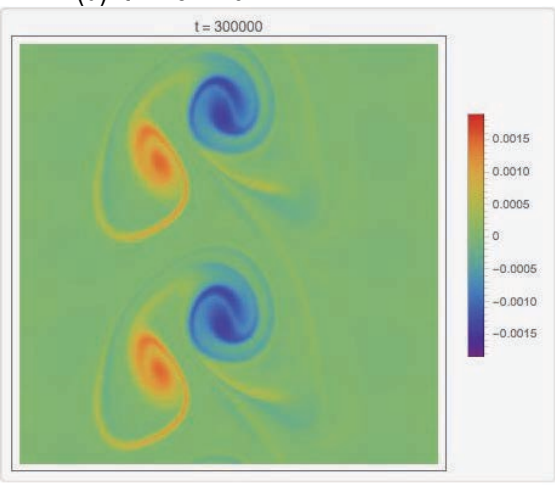

(e) t = 300 x 10^3

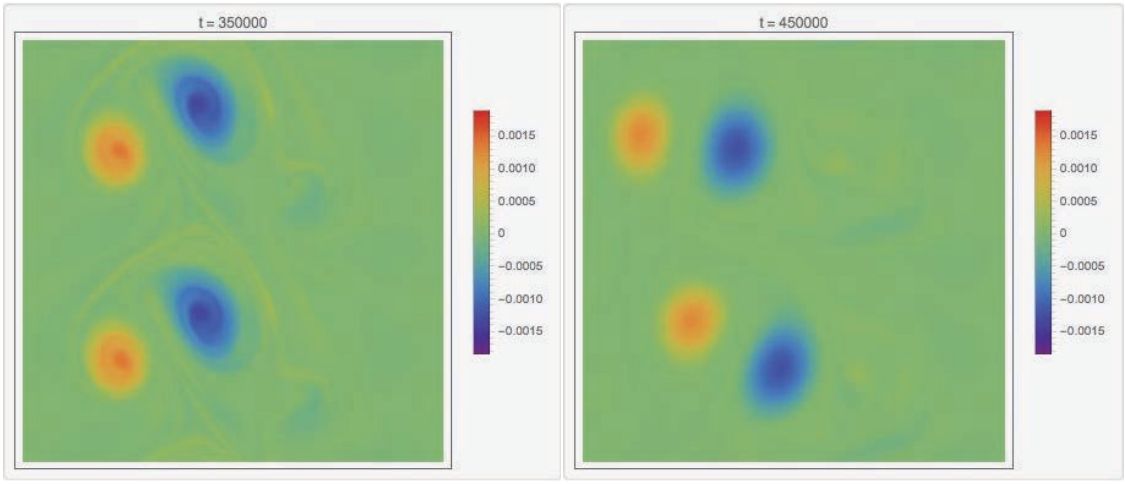

(f) t = 350 x 10^3 (g) t = 450 x 10^3

Fig. 3 The development of the vorticity $\omega(x,y) = \partial_x u_y - \partial_y u_x$ in the *Kelvin-Helmholtz instability of a 2D velocity jet. Grid = 1024², viscosity* $\nu = 10^{-3}$, *mean flow* $U_0 = 0.049$, $\mathrm{Re} = 5\times 10^4$. *The color scheme is held fixed throughout these plots.*

In Fig. 3 we present the development of the Kelvin-Helmholtz instability for a fluid jet with initial velocity profile.

$$u_y(x) = U_0\, sech^2 x \quad , \quad u_x = 0 \tag{16}$$

Because of the sharp changes in slope in the velocity profile, the vorticity consists of 2 counter-streaming layers [the red $\omega > 0$ and the blue $\omega < 0$ in Fig. 3]. The 2D jet is Kelvin-Helmholtz unstable. A 1% periodic perturbation is applied to the velocity field. Each vorticity layer (continuous in y) breaks up into a series of vortex blobs rotating in the same direction, but opposite to those vortex blobs in the other layer. As the instability evolves these vortex blobs start to interact with each other and tear the layer (which was parallel to the y-axis) apart, Fig. 3(d). Since we move into the regime of 2D turbulence, like vortices merge and so by t = 300K we have two sets of two vortex blobs moving throughout space – the jet being destroyed.

One can also consider the energy spectra $E_{tot}(k)$, where the total energy

$$E = \int_0^L d^2x \left(\frac{\mathbf{u}^2}{2} + \frac{\mathbf{B}^2}{2} \right) = \int_0^{k_{max}} dk\, E_{tot}(k) \tag{17}$$

The corresponding energy spectra $E_{tot}(k)$ are shown in Fig. 4

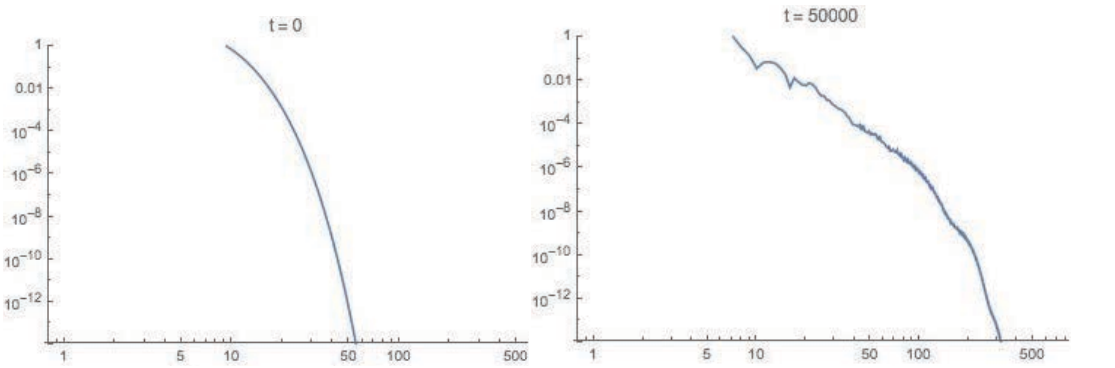

(a) t = 0 *(b) t = 50* x 10^3

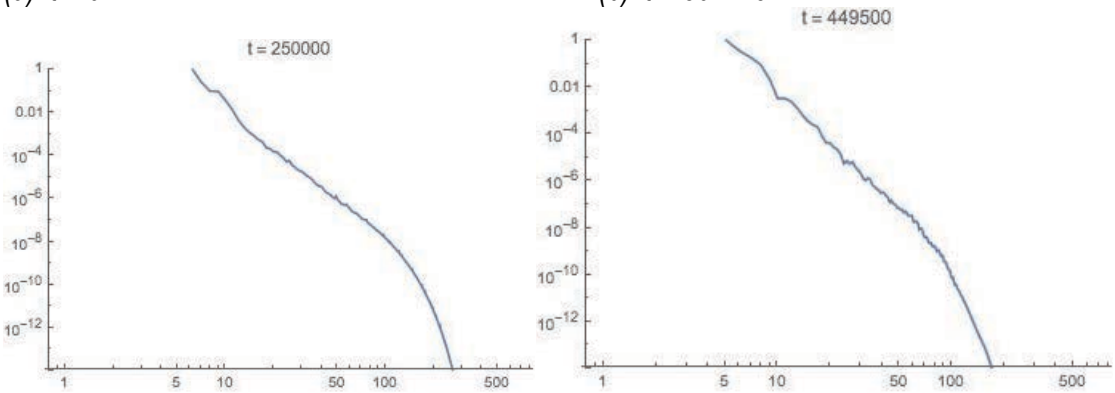

(c) t = 250 x 10^3 *(d) t = 449.5* x 10^3

Fig. 4 Total (Kinetic) energy spectrum $E_{kin}(k)$ *for the Kelvin-Helmholtz instability in 2D Navier-Stokes as a function of the wavenumber* $k = |\mathbf{k}|$. [case of **B** = 0].

We now introduce a relatively strong uniform magnetic field $\mathbf{B}_0 = B_0 \hat{y}$ parallel to the jet flow and see the stabilization of the velocity jet $B_0 / U_0 = 0.25$, Fig. 5. We now see that this magnetic field is sufficiently strong to prohibit the formation of vortex blobs within the vortex layers. While vorticity

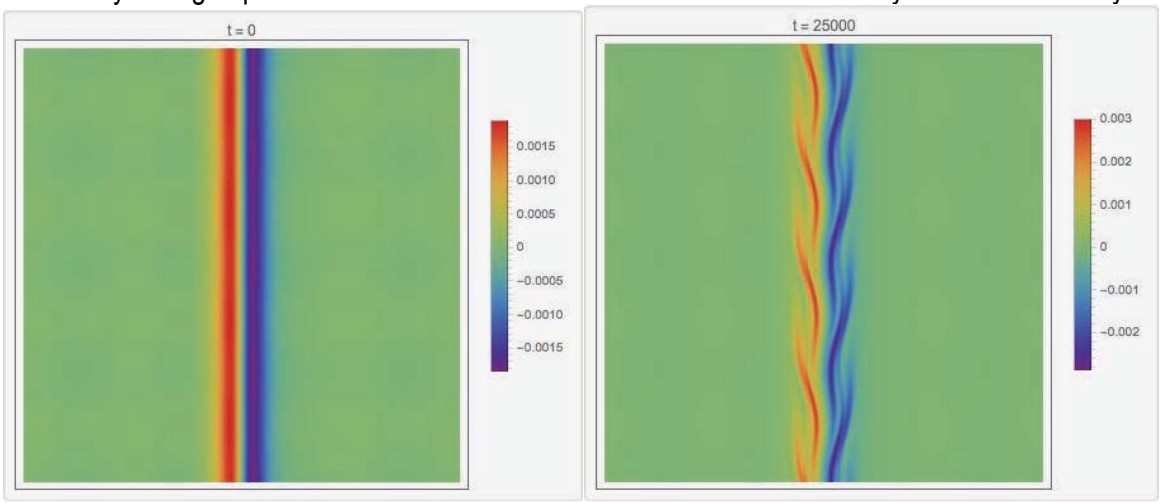

(a) t = 0 *(b) t = 25* x 10^3

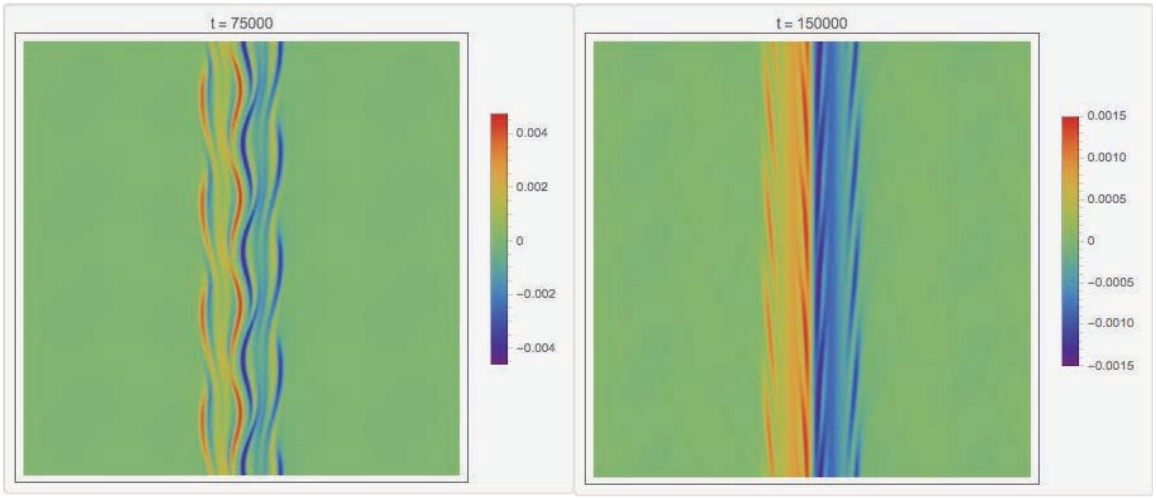

(c) $t = 75 \times 10^3$ *(d)* $t = 150 \times 10^3$

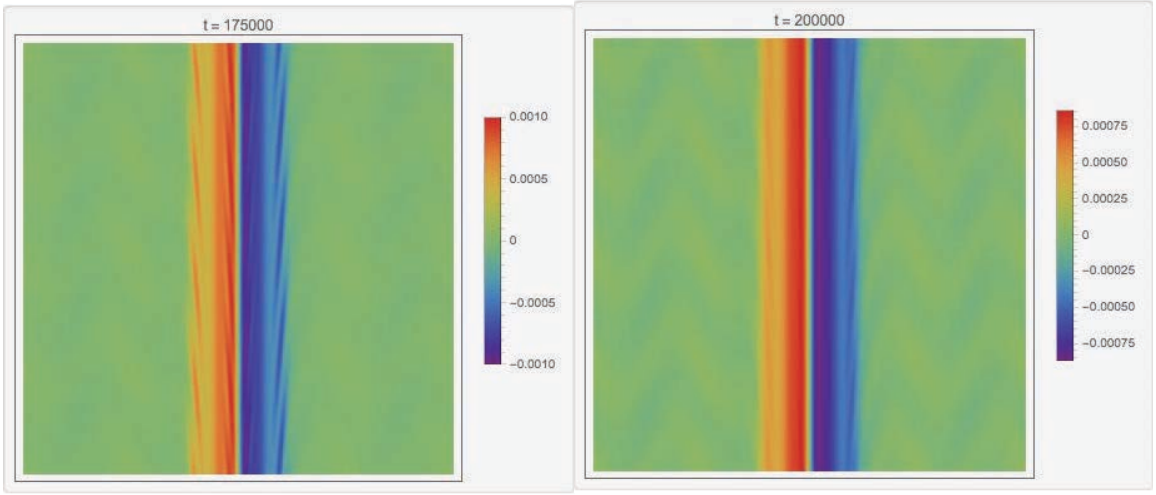

(e) $t = 175 \times 10^3$ *(f)* $t = 200 \times 10^3$

Fig. 5 The stabilization of the velocity jet by a sufficiently strong axial uniform magnetic field for the 9-bit SRT model. Vortex blobs do not form in the vortex layers and the jet retains its basic form but quite strong transient vorticity streaks are formed [c.f. (b)-(d)], but which are then stabilized, resulting in a velocity jet which has somewhat increased in width. The color scheme is adaptive, unlike that for the Navier-Stokes simulation, Fig. 3.

stripes are found within the layers (Fig. 5a), the vortex layers retain their identity albeit being somewhat more diffuse (Fig. 5b).

In Fig. 6 we plot the initial (t = 0) and final (t = 500 x 10^3) jet velocity profiles noticing how the parallel magnetic field stabilizes the jet – but with slight broadening of the profile

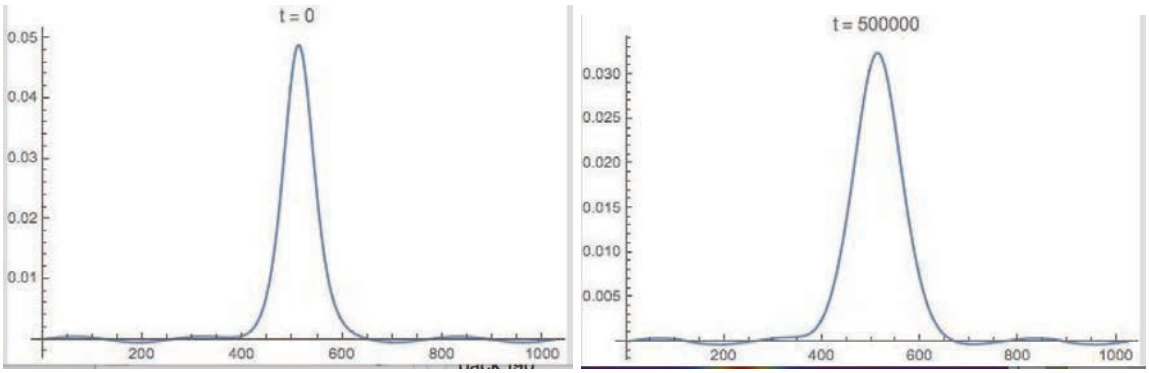

(a) initial jet profile (t = 0) *(b) stabilized jet profile at t = 500* x 10^3

Fig. 6 The velocity profile of the jet stabilized against the Kelvin-Helmholtz instability by a strong axial magnetic field, using the 9-bit SRT model for the magnetic vector distribution functions.

It should be noted that the computational costs (in terms of wallclock time) of the 9-bit SRT model are almost identical to that of the 5-bit MRT models introduced by Dellar [9, 10] and Flint et. al. [6]. The 9-bit MRT model is considerably more expensive [by more than a factor of 50%].

The corresponding total (kinetic + magnetic) energy spectra for the 9-bit SRT model are shown in Fig. 7

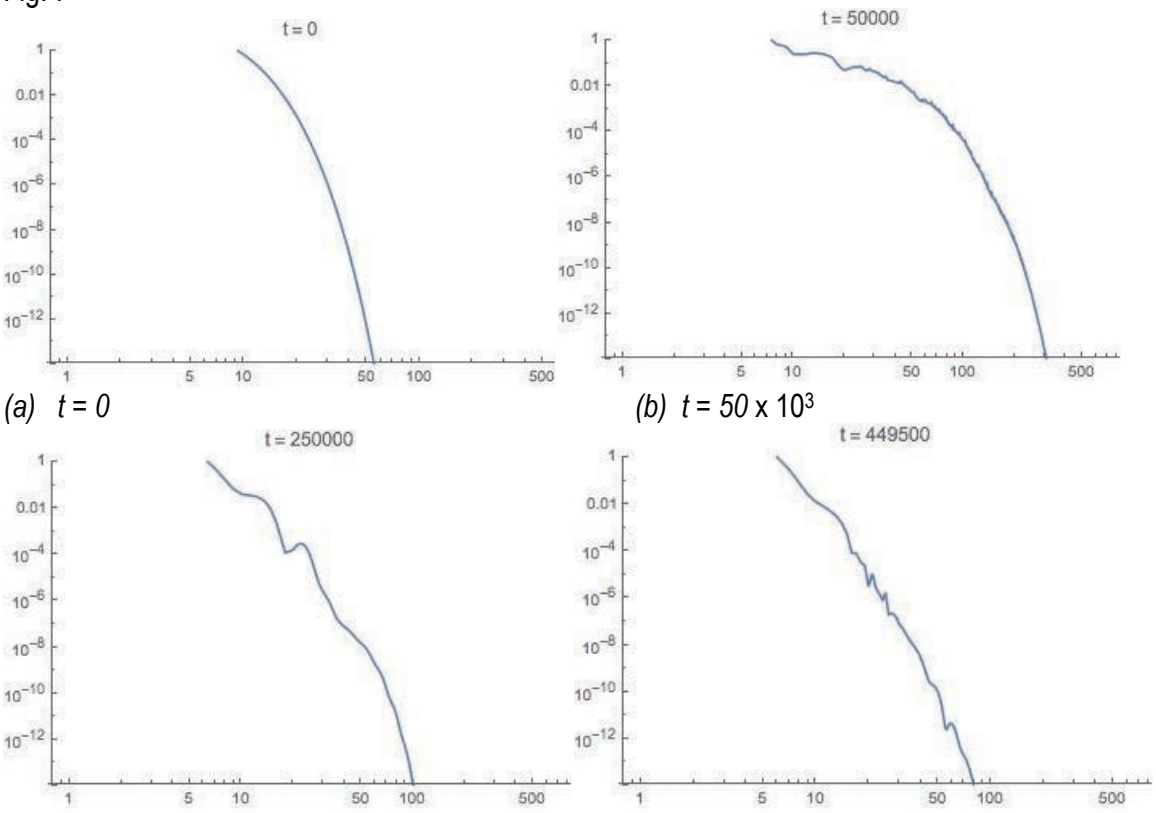

(a) t = 0 *(b) t = 50* x 10^3

(c) t = 250 x 10^3 *(d) t = 449.5* x 10^3

Fig. 7 The total energy spectrum $E_{tot}(k)$ *for the magnetically stabilized velocity jet (9-bit SRT model) as a function of the wavenumber* $k = |\mathbf{k}|$

Except for the early stages ($t < 70 \times 10^3$) there are considerable small scale structures still present in the magnetized velocity jet, but as the stabilization sets in these small scale structures are suppressed. This is evident in Fig. 7(b) with the wave number of excited modes reaching k = 300 (for energy spectra ranges held the same in all plots of Fig. 7). The corresponding stabilization and spectral plots for the standard 5-bit MRT LB-MHD model are basically identical to the 9-bit SRT LB-MHD model for $t < 200 \times 10^3$. However, for times $t > 200 \times 10^3$ numerical instabilities arise in the 5-bit MRT model, but which are not seen in the 9-bit SRT model at these strong magnetic fields $B_0 / U_0 = 0.25$.

6. CONCLUSION

The LB-MHD algorithm is an ideal computational tool as one scales codes to exascale because of its impressive parallelization. This parallelization arises because the 2 major LB-MHD operations: (a) free-streaming distribution function data to nearby spatial nodes (a simple shift), and (b) local collisional relaxation of the distribution functions (requiring only local data at the nodes). Here we have applied the LB-MHD code to study the stabilization of the Kelvin-Helmholtz unstable 2D-fluid jet by an external parallel magnetic field. Since the vector distribution function, as originally introduced by Dellar [2], can recover the magnetic field at its zeroth moment the underlying lattice for 2D problems can be restricted to the simple 5-bit model. This SRT model has then been extended by Dellar [9, 10] and Flint et. al. [6] to MRT where the collision-step is now performed in the moment space of the magnetic distribution function as it is also performed for the moment velocity space so as to take full advantage of the local collisional invariants. In this paper we have examined the consequences of moving to a 9-bit lattice for the magnetic velocity distribution function and applied the model to the stabilization of the Kelvin-Helmholz instability in a fluid jet. Since the strength of the stabilizing axial magnetic field is a critical parameter in the jet stabilization, we have examined the effect of lattice geometry and kinetic collisional relaxation rates on B_{max} before numerical instabilities limit the simulation. We found that B_{max} can be successfully increased by 34% in moving from the 5-bit MRT magnetic lattice to the 9-bit SRT lattice with no loss in the computational wallclock time required. However the further extension to 9-bit MRT magnetic lattice only permitted B_{max} to be 40% greater than the 5-bit MRT while the computational wallclock now increased by over 50%.

The optimal choice of kinetic moments basis is still an open question. Our choice was predicated on making the choice of the next higher order moments – but with our current results on the importance of the 9-bit SRT (which does not require the introduction of a kinetic moment space for the magnetic distribution) it may be a mute point. We have also performed some parameter runs in the choice of the stabilizing moment relaxation rates on achievable B_{max}. With 6 degrees of freedom in the kinetic moment relaxation rates only a somewhat superficial testing was performed. No particularly strong correlations were found. In some cases, forcing strong damping of some of the higher kinetic moments did not lead to stabilization while reducing some led to better results. Again, in light of the important gains in the 9-bit SRT magnetic lattice (at no extra computational costs) this seems to be a secondary issue.

The important question of whether these results will also hold in wall-bounded flows is left for a future study. It is well known that the accuracy and stability of an LB-code is dependent on the treatment of boundary conditions. This would introduce another set of free parameters that would possibly lead to further discussions on improvement in boundary condition implementations. Since

our next major goal is to extend these MHD results from 2D to 3D (in periodic geometry) and examine the differences between 2D and 3D Kelvin-Helmholtz jet stabilization in an axial magnetic field with an eye to moving to magnetic fusion applications where the toroidal magnetic field is an order of magnitude greater than the poloidal field, we are leaving the effect of wall boundary conditions for a later study.

ACKNOWLEDGEMENTS
This work was partially supported by AFOSR and NSF.

REFERENCES
[1] S. Succi, *The Lattice Boltzmann Equation for Fluid Dynamics and Beyond,* Clarendon Press, 2001 - and references therein
[2] P. J. Dellar, "Lattice kinetic schemes for magnetohydrodynamics", J. Comput. Phys. **179**, (2002) 95-126
[3] Lord Kelvin, "Hydrokinetic solution and observations", Phil. Mag. **42**, 362-377 (1871)
[4] S. Chandrasekhar, *Hydrodynamics and Hydromagnetic Stability* (Oxford Univ. Press, Oxford), 1961
[5] D. d'Humieres, I. Ginzburg, M. Krafczyk, P. Lallemand and L-S. Luo, "Multiple-relaxation-time lattice Boltzmann models in three dimensions", Phil. Trans. R. Soc. Lond. A **360,** 437- 451 (2002)
[6] C. Flint, G. Vahala, L. Vahala and M. Soe, "Magnetic field stabilization of a two-dimensional fluid jet: a multiple relaxation lattice Boltzmann simulation", REDS (to be published).
[7] P. J. Dellar, "Moment equations for magnetohydrodynammics", J. Stat. Phys **P06003-22**, (2009)
[8] S. Ansumali, I. V. Karlin and S. Succi, "Kinetic Theory of Turbulence Modeling: Smallness Paameter, Scaling and Microscopic Derivation of Smagorinsky Model", Physica **A338**, 379-394 (2004).
[9] P. J. Dellar, "Electromagnetic waves in lattice Boltzmann magnetohydrodynamics", Europhys. Lett. **90**, 50002 (2010)
[10] P. J. Dellar, "Lattice Botlzmann magnetohydrodynamics with current-dependent resistivity", J. Computat. Phys. **237**, 115-131 (2013).
[11] D. Biskamp, *Magnetic Reconnection in Plasmas, (*Cambridge Univ. Press, Cambridge) 2000.
[12] P. J. Dellar, "Bulk and shear viscosities in lattice Boltzmann equations." Phys. Rev. **E 64** (2001) 031203.